JOURNAL OF MAGNETIC RESONANCE 53, 313–340 (1983)

Evaluation of a New Broadband Decoupling Sequence: WALTZ-16

A. J. SHAKA, JAMES KEELER, AND RAY FREEMAN

Physical Chemistry Laboratory, Oxford University, Oxford, England

Received February 3, 1983

A new scheme for low-power broadband heteronuclear decoupling is described, based on the use of a composite radiofrequency pulse sequence $90°(+X)\ 180°(-X)\ 270°(+X)$, incorporated into a repeated cycle or supercycle. Its principal attribute is that the residual splittings on the observed resonances (usually carbon-13) are very small (less than 0.1 Hz) for a wide range of decoupler offsets (approximately $-B_2 < \Delta B < +B_2$). Existing theories of broadband decoupling are used to calculate the effects of various possible instrumental imperfections on decoupling performance. It is concluded that spatial inhomogeneity of the B_2 field has a perceptible influence near the extremes of the decoupler bandwidth. Only 180° shifts of the radiofrequency phase are used, and the performance is remarkably insensitive to the exact setting of this phase shift. Any decoupler which employs a systematic modulation scheme runs the risk of introducing "cycling sidebands" into the observed spectrum; it is demonstrated that with the proposed sequence these sidebands are very weak, particularly when the decoupling cycle and the signal acquisition processes are not synchronized. As an illustration, the broadband-decoupled carbon-13 spectrum of an aniline derivative is recorded showing natural-abundance carbon-13 satellite signals but no appreciable cycling sidebands. The circuit for a practical implementation of this decoupling sequence is described.

INTRODUCTION

Efficient decoupling of protons while observing carbon-13 spectra has long been an important practical goal in high-resolution NMR. The penalty for inefficiency is a loss of resolution and sensitivity through the introduction of small unresolved residual splittings on the carbon resonances, or overheating of the sample by the radiofrequency field B_2. For several years the accepted techniques for broadband decoupling have been noise modulation (*1*), square-wave modulation (*2*), chirp frequency modulation (*3*), or some variant of these (*4*). Although these methods have proved satisfactory for many applications, the target specifications are being continually raised by the introduction of spectrometers operating at higher magnetic fields with correspondingly wider proton chemical shift ranges. Biological studies are particularly critical owing to the widespread use of high B_0 fields, the ionic nature of many of the solutions, and the sensitivity of many biological samples to heat.

In retrospect it appears that the rationale behind these conventional decoupling methods may have been unsound, often being based on consideration of the Fourier spectrum of the proton irradiation, and it is only recently that general theories for decoupling with modulated irradiation have emerged. The initial progress was made using average Hamiltonian theory (*5*) and led to the introduction of a family of decoupling sequences known as MLEV-4, MLEV-16, etc. (*6–8*). Although this ap-

0022-2364/83 $3.00

proximate treatment provides insight into the operation of the decoupling sequences and suggests rules for building up more efficient "supercycles" (*8–10*), it is cumbersome in its detailed application (*9*) and in general underestimates the effectiveness of the decoupling. Recently Waugh (*11–13*) has developed an elegant general theory based on direct integration of the equations of motion of the coupled spins when the protons are subjected to a repetitive sequence of rotations about tilted effective fields in the rotating reference frame. It predicts the form of the carbon-13 spectrum for any given sequence of proton pulses and any given proton resonance offset, using an exact calculation rather than the power series expansion implicit in the average Hamiltonian theory. This method lends itself to a numerical simulation of the decoupling performance as a function of proton resonance offset, permitting rapid evaluation of any proposed new decoupling sequence. Inspired by the Waugh theory of decoupling, the present paper describes a decoupling sequence (WALTZ-16) that affords several practical advantages.

PRACTICAL REQUIREMENTS FOR DECOUPLING

What constitutes "good" decoupling? For the majority of applications the overriding consideration is the effective decoupling bandwidth for a given radiofrequency power dissipation. Bandwidth in this context is a somewhat arbitrary term; a working definition is the range of proton offsets for which the carbon-13 resonance remains within 80% of the peak height observed in a conventional coherent on-resonance decoupling experiment. In practice this is strongly influenced by the choice of sensitivity enhancement function used on the carbon-13 free induction signal since the resultant line broadening obscures the effect of very small residual splittings. For Lorentzian lines the residual splitting first becomes evident (as a flat top) when the ratio of splitting to full linewidth reaches about 60%. The peak height falls to 80% of its maximum just before splitting-to-linewidth ratio reaches 50%. For the more routine applications of carbon-13 spectroscopy, where digital resolution is often a limiting factor, a linewidth of the order of 2 Hz would be acceptable and residual splittings of the order of 1 Hz could be tolerated. On the other hand, there are more demanding experimental situations that might require a resolving power as much as an order of magnitude higher, and then careful attention must be paid to holding residual splittings below about 0.1 Hz. Not all decoupling schemes achieve this, although the Waugh sequences (*11, 13*) and WALTZ-16 do meet these stringent resolution requirements. The earlier MLEV sequences fall short of this high standard, partly because of instrumental shortcomings. Sequences which employ 90° phase shifts of the radiofrequency pulses are often quite critically dependent on the accuracy of the phase shifts. Experiments and computer simulations both indicate that deviations of as little as 0.5° in the orthogonality or in the phase inversion can introduce appreciable variations in the quality of the decoupling. In contrast, sequences which employ only 180° phase shifts are very much less sensitive to small phase errors.

A second desirable property of a broadband decoupler is a tolerance of errors in the pulse flip angles. It is not a simple matter to calibrate the B_2 intensity accurately; the usual method is to measure the residual splittings of the carbon-13 resonance with coherent irradiation of the protons at a series of known offsets for a sample of

known J_{CH}. The calibration may well have an inaccuracy of a few percent. A more insidious difficulty arises from the spatial inhomogeneity of the radiofrequency field B_2. Even if the decoupler coil shape is designed for a homogeneous B_2 field, the presence of the receiver coil will tend to distort this. Sample spinning cannot be relied upon to average out the effects of radiofrequency inhomogeneity for the types of decoupling experiment described below. Fortunately sample regions in very low B_2 fields are also only weakly coupled to the receiver coil and contribute relatively little to the overall signal intensity. A decoupling sequence should therefore be designed to be relatively insensitive to small variations in the pulse flip angle, and most sequences examined to date appear to have some degree of compensation for pulse length errors. Nevertheless, B_2 inhomogeneity is certainly one of the factors responsible for the degradation of decoupling performance near the shoulders of the offset-dependence curve. At large proton offsets, regions of the sample which experience abnormally low B_2 fields exhibit residual splittings that are often large compared with the carbon-13 linewidth. Intensity is thereby lost from the central peak and redistributed into the skirts of the line. Occasionally this effect can be so marked that the narrow decoupled carbon-13 line sits in the centre of a strong broad pedestal. This has been observed (*14*) under certain conditions of square-wave modulation, where B_2 inhomogeneity effects are rather poorly compensated.

At the low B_2 levels employed in these experiments, the repetition period of the decoupling sequence can be quite long, of the order of 5 to 50 msec. Sampling rates for carbon-13 spectroscopy may range from 5 to 25 kHz (with quadrature detection) so it is clear that carbon-13 data points must be acquired many times within the proton irradiation period. Optimum decoupling is achieved only at the end of each supercycle, with near-optimum conditions at the end of the intermediate cycles. The process is formally analogous to the refocusing effect responsible for the formation of spin echoes, or line narrowing by spinning the sample; in both cases the periodicity remains undetected if the sampling is synchronized with the cycling rate. When the sampling rate is fast compared with the cycling rate, a spurious modulation is detected on the free induction signal at the cycling rate and its harmonics. After Fourier transformation this is converted into sidebands of the carbon-13 resonance, reminiscent of the well-known spinning sidebands. When the decoupling is efficient, these sidebands are very weak. They are further attenuated (but not eliminated) by the process of time averaging, provided that the sampling of the carbon-13 signal is not synchronized with the proton pulse cycle. One simple way to achieve this desynchronization is to employ a hard-wired proton decoupler running from an independent internal clock (*15*). These "cycling sidebands" are probably the principal factor determining how low a radiofrequency field can be used for decoupling. A low B_2 field entails a low cycling rate, with appreciable deviations of the observed free induction signal from the ideal, fully decoupled, signal. The resulting proliferation of cycling sidebands may prove unacceptable, particularly in experiments where weak resonances must be identified in the presence of nearby strong resonances. The study of carbon–carbon coupling in natural abundance samples is a case which springs to mind.

The desirable properties of a broadband decoupler may therefore be summarized.

(a) Wide effective bandwidth for a given radiofrequency power dissipation.
(b) Residual splittings small compared with the width of the resonance lines of the observed nucleus.
(c) Insensitivity to small errors in pulse length and to the spatial inhomogeneity of the B_2 field.
(d) Only low-intensity "cycling sidebands."
(e) Insensitivity to small errors in the relative phases of the radiofrequency channels.
(f) Programming simplicity.

These criteria have been arranged in approximate order of importance, although, of course, a particular application may make heavy demands on one decoupler feature at the expense of the others.

COMPOSITE PULSE DECOUPLING

The earliest decoupling experiments made use of a single coherent radiofrequency field B_2. They thus enjoyed an important advantage because the decoupled spectrum could be calculated analytically by a simple theory (*16, 17*). For the case of a single proton coupled to a single carbon-13 spin, it is sufficient to examine the effective fields B_+ and B_- acting on the two proton (satellite) lines in a reference frame rotating in synchronism with B_2.

$$\gamma B_+/2\pi = [(\nu_2 - \nu_H + J_{CH}/2)^2 + (\gamma B_2/2\pi)^2]^{1/2}$$
$$\gamma B_-/2\pi = [(\nu_2 - \nu_H - J_{CH}/2)^2 + (\gamma B_2/2\pi)^2]^{1/2} \quad [1]$$

where ν_2 is the frequency of the decoupling irradiation and ν_H is the proton chemical shift. It is easily shown that the residual splitting of the carbon-13 resonance is $\gamma[B_+ - B_-]/2\pi$ Hz, and that there are two symmetrically disposed weak satellite responses separated by $\gamma[B_+ + B_-]/2\pi$ Hz, corresponding, in the limit of efficient decoupling, to two-quantum processes. If the directions of the effective fields acting on the two satellite lines are represented by the unit vectors $\mathbf{n}_+$ and $\mathbf{n}_-$ (anticipating the nomenclature used below) then the main lines have relative intensities $(1 + \mathbf{n}_+ \cdot \mathbf{n}_-)/2$ while the satellites have relative intensities $(1 - \mathbf{n}_+ \cdot \mathbf{n}_-)/2$. A zero residual splitting is achieved at the unique condition $\nu_2 = \nu_H$ for a strong irradiation field $\gamma B_2/2\pi \gg J_{CH}$. At all other offsets there is an appreciable residual splitting, although this is small if $\gamma B_2/2\pi$ is large compared with the proton offset in hertz.

The aim of the new broadband decoupling methods is to impose some time-dependent radiofrequency field on the protons such that the time-averaged effect is essentially the same on the two proton (satellite) lines (*11–13*), thus paralleling the behavior of coherent decoupling at exact resonance. The key difference is that this condition should hold to a good approximation over a wide range of proton offsets, not just near the exact resonance condition.

A continuous radiofrequency field applied at exact proton resonance with $\gamma B_2/2\pi \gg J_{CH}$ induces a continuous nutation of the proton vectors about the X axis of the rotating frame. This may be thought of as a repeated sequence of proton

inversion pulses applied with no interpulse intervals. Thus if a sequence could be found which behaved like an ideal 180° proton pulse even at appreciable offsets from resonance, this should provide a suitable basic element for a broadband decoupling sequence. Composite pulse sandwiches are known which have this property; three such sequences are considered here:

$$R_1 = 90°(X)\ 240°(Y)\ 90°(X) \quad [2]$$

$$R_2 = 90°(X)\ 180°(Y)\ 90°(X) \quad [3]$$

$$R_3 = 90°(X)\ 180°(-X)\ 270°(X). \quad [4]$$

The parentheses refer to the relative radiofrequency phases. The pulses are written in terms of the nominal flip angles (the rotation angles at exact resonance) neglecting the effects of spatial inhomogeneity of the B_2 field.

Cycles

The next question is how to assemble spin inversion elements into an effective decoupling sequence. Simple repetition, $(R)_n$, is not sufficient, since it shares part of the drawbacks of continuous wave decoupling. It is necessary to make use of an equal number of elements $\bar{R}$, derived from R by inversion of all the radiofrequency phases. Levitt has shown (*6*) that the basic sequence must be of the form $(RR\bar{R}\bar{R})_n$ rather than the alternative $(R\bar{R}R\bar{R})_n$, and this "MLEV-4" decoupling scheme has been justified theoretically (*6, 9*) and demonstrated experimentally. A possible rationalization of this choice of ordering may be made by considering the case of simple 180° pulses, applied at a finite offset from resonance. The sequence $180°(+X)\ 180°(+X)$ returns a magnetization vector to a point close to its initial position, whereas the sequence $180°(+X)\ 180°(-X)$ takes such a vector much farther away, as can be appreciated from the calculated trajectories of Fig. 1. A sequence which returns a typical magnetization vector exactly to its initial condition (neglecting relaxation) is said to be *cyclic*. Thus RR is more cyclic than $R\bar{R}$, and by similar reasoning $RR\bar{R}\bar{R}$ is much more cyclic than $R\bar{R}R\bar{R}$. It has been shown (*11*) that good cyclicity goes hand-in-glove with decoupling efficiency.

The Waugh Theory (11–13)

This theory assumes that the coupling between protons is weak in comparison with the coupling between protons and carbon-13 (so solid state and liquid–crystal situations are not necessarily covered). There is the further assumption that carbon–carbon coupling is neglected, although experiments reported below suggest that this is an unnecessary restriction. The treatment starts from the premise that the protons are subjected to a sequence of radiofrequency pulses in a periodic manner with repetition period t_p seconds. The sequence is considered as a small number of consecutive "states" during which the Hamiltonian is time independent. Within a given state the motion of the two proton (satellite) lines is represented by pure rotations about the appropriate effective fields B_+ and B_- as in the theory of continuous-wave

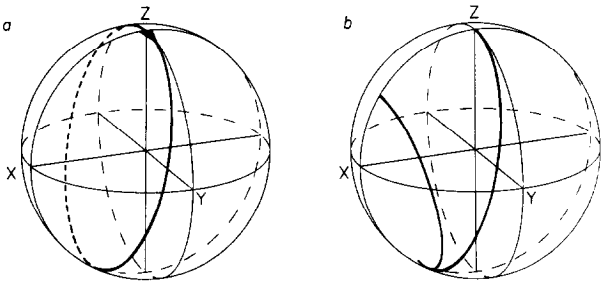

FIG. 1. Magnetization trajectories calculated for (a) 180°(+X) 180°(+X) and (b) 180°(+X) 180°(−X) at a resonance offset $\Delta B = 0.25\, B_2$. Sequence (a) causes only a small overshoot past one complete revolution (as far as the tip of the arrow). It is therefore much closer to the cyclic condition than sequence (b) which leaves the magnetization vector a considerable distance from the +Z axis. It follows that 180°(+X) 180°(+X) 180°(−X) 180°(−X) is more nearly cyclic than 180°(+X) 180°(−X) 180°(+X) 180°(−X).

decoupling. The overall result of a sequence of several consecutive rotations is calculated by explicit matrix multiplication and represented by a net rotation

$$\Omega_{\pm} = \exp(i\beta_{\pm}\mathbf{n}_{\pm} \cdot \mathbf{I}) \qquad [5]$$

where β_+ and β_- are the angles through which the two proton satellites rotate and $\mathbf{n}_+$ and $\mathbf{n}_-$ represent the respective rotation axes.

Since the proton irradiation is periodic, it is sufficient to calculate the carbon-13 free induction signal at the end of one period, assuming (for the time being) that the sampling operation occurs in synchronism. At this point the carbon-13 signal is given by

$$f(t_p) = 0.5(1 + \mathbf{n}_+ \cdot \mathbf{n}_-) \cos[(\beta_+ - \beta_-)/2] + 0.5(1 - \mathbf{n}_+ \cdot \mathbf{n}_-) \cos[(\beta_+ + \beta_-)/2]. \qquad [6]$$

The frequency-domain spectrum consists of four lines. There are two "main" lines centered about the carbon-13 shift with a splitting $(\beta_+ - \beta_-)/2\pi t_p$ Hz, and relative intensities $(1 + \mathbf{n}_+ \cdot \mathbf{n}_-)/2$. These are flanked by two weak outer lines with a splitting $(\beta_+ + \beta_-)/2\pi t_p$ Hz and relative intensities $(1 - \mathbf{n}_+ \cdot \mathbf{n}_-)/2$. The situation is thus formally analogous to that of continuous-wave decoupling described above. In the majority of applications the B_2 field is sufficiently strong compared with J_{CH} that the angle between the two axes $\mathbf{n}_+$ and $\mathbf{n}_-$ is small, so the main lines have essentially all the intensity and the outer lines may be neglected. The formal condition for good decoupling is that $(\beta_+ - \beta_-)$ be small. This is generally true if β varies only slowly with proton resonance offset $\omega = \gamma\Delta B$. In practice a small residual splitting is ensured by keeping both β_+ and β_- small, so the difference is always small. In this limit where β changes only slowly, it is useful to define a scaling factor given by the derivative

$$\lambda = (1/t_p)\, d\beta/d\omega. \qquad [7]$$

The residual splitting is then given by λJ_{CH} to a very good approximation. The offset dependence of λ is readily computed and provides a good test of any proposed new decoupling sequence.

This argument has assumed that the carbon-13 sampling operation occurs only at the end of each proton cycle. Waugh (*11, 12*) has shown that since β is not affected by cyclic permutation of any part of the proton pulse sequence, sampling may occur at any point in the cycle, provided that it is always the same point in each cycle. In practice even this latter condition may be relaxed since asynchronous acquisition merely introduces a very weak modulation onto the carbon-13 free induction signal.

Supercycles

Improvements in the cyclicity of a sequence have the effect of enhancing the decoupling performance. Consequently, the next step is to examine ways in which this net rotation Ω might be compensated by an approximately equal and opposite rotation generated by a subsequent modified sequence. There are two types of modification possible. The first converts the primitive cycle C into the phase-inverted cycle $\bar{C}$. This keeps $\beta_\pm$ unchanged but reverses the X and Y coordinates of the rotation axis $\mathbf{n}_\pm$. The second possible modification involves a cyclic permutation of some segment of the cycle, for example one element:

$$RR\bar{R}\bar{R} \rightarrow R\bar{R}\bar{R}R. \qquad [8]$$

In general, if an odd number of elements is permuted, the new sequence is designated P. Cyclic permutation of a perfect 180° pulse is equivalent to reversing the Z coordinate of the rotation axes $\mathbf{n}_\pm$; in practice the pulse imperfection has to be taken into account. The rotation angles $\beta_\pm$ are not affected by cyclic permutation or phase inversion.

It is therefore evident that an approximate compensation for the imperfection of the cycle C may be achieved in the *supercycle* CP and then further compensation obtained by combining this with its phase-inverted counterpart $\bar{C}\bar{P}$ to give the supercycle $CP\bar{C}\bar{P}$. As an example, the primitive cycle MLEV-4,

$$C = RR\bar{R}\bar{R} \qquad [9]$$

is converted to MLEV-8 by combining it with the permuted sequence P to give the supercycle

$$S_1 = RR\bar{R}\bar{R}\ \bar{R}RR\bar{R}. \qquad [10]$$

The next stage of refinement utilizes the phase-inverted sequences $\bar{C}$ and $\bar{P}$, generating the MLEV-16 supercycle

$$S_2 = RR\bar{R}\bar{R}\ \bar{R}RR\bar{R}\ \bar{R}\bar{R}RR\ R\bar{R}\bar{R}R. \qquad [11]$$

The four rotations corresponding to the four imperfect cycles generate four small arcs near the $+Z$ axis of the rotating frame, forming an almost closed loop. There is one such loop for each proton satellite line (H_+ and H_-). The additional rotation required to close such a loop corresponds to the overall rotation angle β_+ or β_- of the supercycle. What matters for good decoupling performance is that the *difference* $\beta_+ - \beta_-$ should be as small as possible, and this is ensured by making both angles very small. Figure 2 maps out two typical MLEV-16 loops for H_+ and H_- to illustrate this point. It is clear that the supercycle is much nearer to cyclicity than the individual

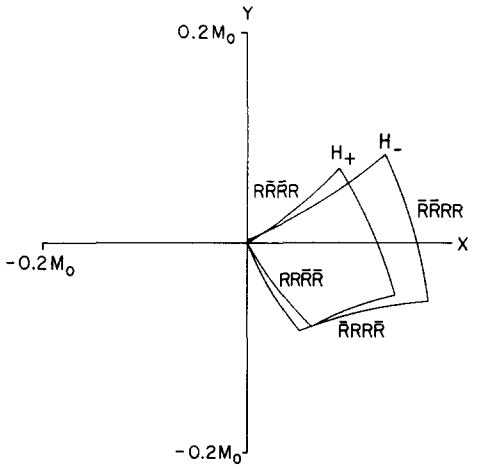

FIG. 2. Trajectories representative of the four component cycles of the MLEV-16 supercycle projected onto the XY plane. The excursions are all small and close to the $+Z$ axis (only a fifth of the unit sphere is shown). There is one trajectory for each proton satellite line (H_+ and H_-). Each arc represents the deviation of the MLEV-4 sequence from exact cyclicity, while the very small residual arc required to close the loop represents the deviation of the MLEV-16 supercycle from cyclicity.

MLEV-4 cycles, and since *both* loops are almost closed, the decoupling performance is enhanced.

This was the first supercycle to be demonstrated experimentally (*7*). Its extension involves the cyclic permutation of one spin inversion element R from the end to the beginning of the sequence S_2, and combination with S_2, giving MLEV-32

$$S_3 = RR\bar{R}\bar{R}\ \bar{R}RR\bar{R}\ \bar{R}\bar{R}RR\ R\bar{R}\bar{R}R\ RRR\bar{R}\ \bar{R}\bar{R}RR\ \bar{R}R\bar{R}R\ RR\bar{R}\bar{R}. \quad [12]$$

Further improvement is brought about by combination with the corresponding phase-inverted sequence, giving the supercycle MLEV-64

$$S_4 = RR\bar{R}\bar{R}\ \bar{R}RR\bar{R}\ \bar{R}\bar{R}RR\ R\bar{R}\bar{R}R\ RRR\bar{R}\ \bar{R}\bar{R}RR\ \bar{R}R\bar{R}R\ RR\bar{R}\bar{R}$$
$$\bar{R}\bar{R}RR\ R\bar{R}\bar{R}R\ RR\bar{R}\bar{R}\ \bar{R}RR\bar{R}\ \bar{R}\bar{R}\bar{R}R\ RR\bar{R}\bar{R}\ RRR\bar{R}\ \bar{R}\bar{R}RR. \quad [13]$$

There is an important alternative to cyclic permutation of a 180° pulse. The effectiveness of a given cycle is unaltered by cyclic permutation of *any part* of the cycle; it need not be a complete spin inversion element. Waugh (*11, 13*) has demonstrated the utility of permuting a 90° pulse from one end of the cycle to the other. This maintains $\beta_\pm$ unchanged but rotates the axes $\mathbf{n}_\pm$ through approximately 90°, bringing them approximately into the XY plane. If the permuted cycle M is combined with $\bar{M}$, compensation for pulse imperfections is achieved in the supercycle $M\bar{M}$. A particular advantage of this procedure is that the 90° pulse is only required to convert Z magnetization into XY magnetization, the phase in the XY plane being immaterial. Judged by this mild criterion, a 90° pulse is largely self-compensating up to offsets ΔB approximately equal to B_2 (*18–20*). The procedure is therefore to

devise a cycle C which corresponds to an overall rotation about an axis near $+Z$, convert this by permuting a 90° pulse into a new cycle M which has its rotation axis close to the XY plane, and then combine M with $\bar{M}$. This is the method adopted below for the WALTZ-16 decoupling sequence.

In general the nature of the residual imperfections of a given cycle or supercycle determines whether a 180° pulse or a 90° pulse should be cyclically permuted in the next stage of refinement. Eventually further expansion becomes unnecessary when the carbon-13 residual splittings are much smaller than the instrumental linewidth. Performance is even degraded for extensive supercycles (*9*) since there are some kinds of imperfections, for example, motion through the inhomogeneous B_2 field, which cannot be corrected by this procedure.

While supercycles compensate moderate imperfections of the basic spin-inversion elements, they are powerless to correct gross imperfections. The latter intervene when the tilt angle of the effective radiofrequency field (arctan $\Delta B/B_2$) exceeds about 45°, where the self-compensating action of the composite pulse deteriorates very rapidly. Thus, for the sequences described above, the effective decoupling bandwidth is determined principally by the bandwidth for spin inversion; more sophisticated extensions of the supercycle improve this bandwidth only gradually. Hence the importance of choosing a good basic element R. On the other hand, moderate imperfections are readily compensated by the operation of the supercycle. For example, the composite pulse R_1 was originally selected because its offset-dependence curve is very flat in the region

$$-0.5B_2 < \Delta B < +0.5B_2. \qquad [14]$$

It was later replaced by the sequence R_2, which, although there were appreciable undulations in the offset-dependence curve, nevertheless covered the wider range

$$-B_2 < \Delta B < B_2. \qquad [15]$$

Computational Considerations

Numerical calculations of decoupling performance and simulation of decoupled spectra can be time-consuming operations unless certain precautions are taken. These calculations were carried out on a Data General Eclipse S/200 computer using double-precision arithmetic throughout. The 2×2 complex representation of rotation operators was used, advantage being taken of its unitary form to halve the number of multiplications. For decoupling sequences derived by cyclic permutation and phase inversion, the computational time was reduced by an order of magnitude by grouping the sequence into subcycles rather than by brute-force multiplication. Cyclic permutation is a unitary transformation, and phase inversion can be accomplished by a sign change of the R_{12} and R_{21} matrix elements. In this fashion the MLEV-64 supercycle may be simulated with 13 matrix multiplications rather than 192. For a long decoupling sequence at 500 offset increments, a typical computation time would be about 0.5 sec. On the other hand, calculations which take into account the spatial distribution of B_2 fields require several minutes.

A second difficulty arises with numerical instabilities. For sequences that are close

to exact cyclicity, the net rotation angle β can be very small. If it is computed from the formula

$$\beta = 2 \cos^{-1} (\mathrm{Re}\{R_{11}\}) \quad [16]$$

even double-precision arithmetic can introduce appreciable round-off errors for small values of β. It is therefore preferable to compute β from

$$\beta = 2 \sin^{-1} [(\mathrm{Im}\{R_{11}\}^2 + R_{12}^* R_{12})^{1/2}] \quad [17]$$

which deals adequately with small values of β. At some points in the offset-dependence curve, β passes through zero and one of the rotation axes $\mathbf{n}_+$ or $\mathbf{n}_-$ becomes undefined. This difficulty is overcome by forcing $\mathbf{n}_\pm$ to be smoothly varying functions of offset, and then interpolating. This also removes any ambiguity about the sign of β.

THE "WALTZ" SEQUENCES

When the performance of the MLEV sequences is examined under very high resolution conditions, residual splittings as high as 0.2 to 0.4 Hz can be discerned at certain proton offsets. It is also observed that the details of the decoupling behavior depend rather critically on the settings of the relative phases of the four radiofrequency channels ($+X$, $+Y$, $-X$, and $-Y$). Although in many spectrometers these channels are orthogonal within better than 1°, and although it is quite feasible to set up tuning circuits for a much finer adjustment, there are no obvious simple methods for independent calibration of the three 90° relative phase shifts, so this phase sensitivity is a serious practical inconvenience.

These observations are confirmed by computer simulation of the decoupling performance. As an example, Fig. 3 compares the offset dependence curve for the MLEV-64 sequence for (a) exact orthogonality, and (b) a 0.5° misadjustment of the $-X$ channel with respect to the other three. For the shorter supercycles, a small phase misset is not necessarily deleterious, since it may act to improve the cyclicity of a slightly imperfect sequence (*12*), but then the expansion to the next supercycle would require a readjustment of the phase. It should be emphasized that these considerations are unimportant for routine carbon-13 spectroscopy where line broadenings of 1 or 2 Hz are imposed on the observed spectrum, but are only a cause for concern under very high resolution conditions.

This sensitivity to phase error arises with sequences which involve 90° phase shifts, but is virtually absent with sequences which only shift the radiofrequency phase in 180° steps. For example, the performance of the decoupling schemes proposed by Waugh (*11, 13*) is readily shown to be insensitive to errors in the 180° phase shift as large as 10°. Unfortunately these sequences employ a basic cycle $RR\bar{R}\bar{R} = 360°(+X)\ 360°(-X)$, which has only limited compensation for offset effects, and thus cover only a relatively narrow proton bandwidth.

These practical considerations provided the impetus for a search for an alternative composite inversion element which would use only 0 and 180° radiofrequency phases. The other decoupling criteria remain the same, in particular the crucial bandwidth requirement. The starting point is the self-compensating property of a simple 90° pulse (*18–21*). An off-resonance 90° pulse converts Z magnetization into XY mag-

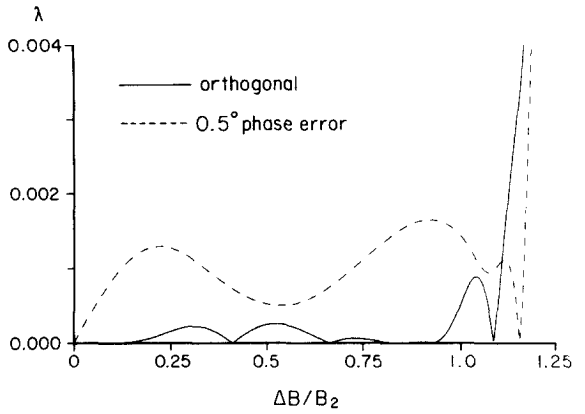

FIG. 3. Sensitivity of the MLEV-64 sequence to errors in the radiofrequency phase shifts. A computer simulation of the scaling factor λ against offset parameter for exactly orthogonal phases and the case where one channel ($-X$) has been deliberately misset by 0.5°. A scaling factor $\lambda = 0.004$ corresponds to a residual splitting of 0.8 Hz if $J = 200$ Hz.

netization with only a small residual Z component, but creates a relatively large dephasing of the vectors in the XY plane, depending almost linearly on offset. It is readily shown that the residual Z component of magnetization is given by

$$M_Z = M_0[\sin^2 \theta + \cos^2 \theta \cos \alpha] \quad [18]$$

where $\alpha = (\pi/2) \sec \theta$ where θ is the tilt of the effective field. A better appreciation of the expression can be obtained by expanding sec θ to second order in θ, which gives

$$M_Z = M_0[\sin^2 \theta - \sin (\pi\theta^2/4)]. \quad [19]$$

This shows that there are no first-order terms in θ and that the leading second-order term is quite small. By contrast, a 180° pulse leaves a Z component of magnetization (to second order)

$$M_Z \cong -M_0[1 - 2 \sin^2 \theta] \quad [20]$$

where the error term is an order of magnitude larger.

If such an off-resonance 90° trajectory could be combined with a subsequent "90°" trajectory for which the dephasing effect were reversed, a compensated spin inversion element would be created. Figure 4 illustrates how this might be achieved with a hypothetical "reversed precession" 90° pulse about the $-X$ axis, written as $[90°(-X)]^{-1}$. (This could be achieved by exact reversal of the sign of the proton resonance offset, but this is not a practical solution for a spectrum of many lines.)

One possible approximation to such a reversed precession 90° pulse is a $270°(+X)$ pulse, based on the approximations

$$360°(+X) \cong \mathbb{1}$$

$$90°(+X)\ 270°(+X) \cong \mathbb{1}$$

$$270°(+X) \cong [90°(+X)]^{-1}. \quad [21]$$

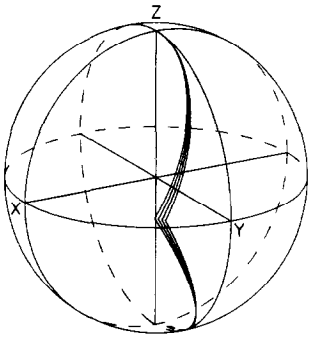

FIG. 4. Magnetization trajectories calculated for a 90°(+X) pulse followed by a hypothetical "reversed precession" 90° pulse about the $-X$ axis. A family of four trajectories is shown near the condition $\Delta B = 0.5\ B_2$. This combination of pulses serves as a 180° pulse compensated for resonance offset effects.

This becomes a less and less satisfactory approximation as the offset increases, the increased effective field causing an overshoot of the $-Y$ axis. An alternative starting point is the approximation

$$270°(-X)\ 270°(+X) \cong \mathbb{1}. \qquad [22]$$

This is not a particularly good approximation at intermediate offsets, but as it passes through the condition $\Delta B = 0.88\ B_2$ it becomes exact again because the actual precession angles are then 360° and magnetization returns to the $+Z$ axis. Another way to write this expression is

$$180°(-X)\ 270°(+X) \cong [90°(-X)]^{-1} \qquad [23]$$

and a self-compensating pulse can be constructed (*18*)

$$R_3 \cong 90°(+X)\ [90°(-X)]^{-1} \cong 90°(+X)\ 180°(-X)\ 270°(+X). \qquad [24]$$

In the shorthand notation introduced by Waugh (*11, 13*) this is written in terms of the number of nominal 90° pulses, a bar denoting phase inversion

$$R_3 = 1\,\bar{2}\,3. \qquad [25]$$

This can be shown to be a good spin inversion sequence by calculating the trajectories on the unit sphere (Fig. 5) for suitable resonance offsets. From these diagrams it is evident that the compensation, which is of course exact at resonance, deteriorates with offset but improves again near the condition $\Delta B = 0.88\ B_2$. Near this condition $1\bar{2}$ is a good inversion element and the last pulse is essentially redundant, causing an almost complete revolution about the effective field vector. However, near resonance the third pulse is essential to the compensation. In all cases the magnetization vector is taken from the $+Z$ axis and carried to a point not too far removed from the $-Z$ axis. The spin inversion efficiency is displayed as a function of offset in Fig. 6.

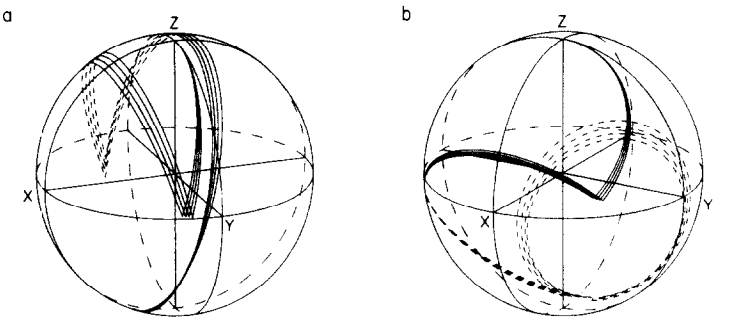

FIG. 5. Magnetization trajectories calculated for the spin inversion sequence $R = 1\bar{2}3$. (a) For small offsets from resonance (near $\Delta B = 0.25\ B_2$) the compensation is only moderate. (b) For offsets $\Delta B/B_2$ between 0.75 and 0.88, the first two pulses achieve the spin inversion and the last pulse merely rotates the magnetization through 360° about the tilted effective field.

This element may then be used to set up a primitive sequence (WALTZ-4)

$$R\bar{R}\bar{R}R = 1\bar{2}3\ 1\bar{2}3\ \bar{1}\bar{2}\bar{3}\ \bar{1}\bar{2}\bar{3}. \qquad [26]$$

The decoupling efficiency of WALTZ-4 can be calculated numerically as a function of proton resonance offset (Fig. 7).

The WALTZ-4 sequence is almost cyclic; the deviation from true cyclicity is represented by an overall rotation through a small angle β about an axis $\mathbf{n}_\pm$ close to the $+Z$ axis. The next stage of the expansion uses a cyclic permutation of a 90°($+X$) pulse from the beginning to the end of the sequence. This has the effect of rotating $\mathbf{n}_\pm$ through the same angle, and since the 90° pulse is self-compensating, it brings $\mathbf{n}_\pm$ almost into the XY plane. The new sequence is then combined with its phase-inverted counterpart to give WALTZ-8

$$K\bar{K}\bar{K}K = \bar{2}4\bar{2}3\bar{1}\ 2\bar{4}2\bar{3}1\ \ 2\bar{4}2\bar{3}1\ \bar{2}4\bar{2}3\bar{1}. \qquad [27]$$

This has been written in a form which combines together any contiguous pulses of

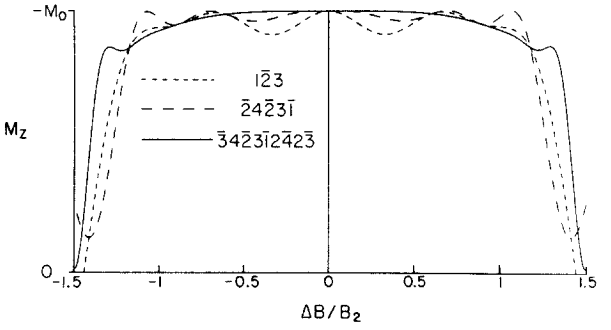

FIG. 6. Efficiency of spin inversion calculated for the sequences $R = 1\bar{2}3$, $K = \bar{2}4\bar{2}3\bar{1}$ and $Q = 3\bar{4}2\bar{3}1\bar{2}4\bar{2}3$ as a function of the offset parameter.

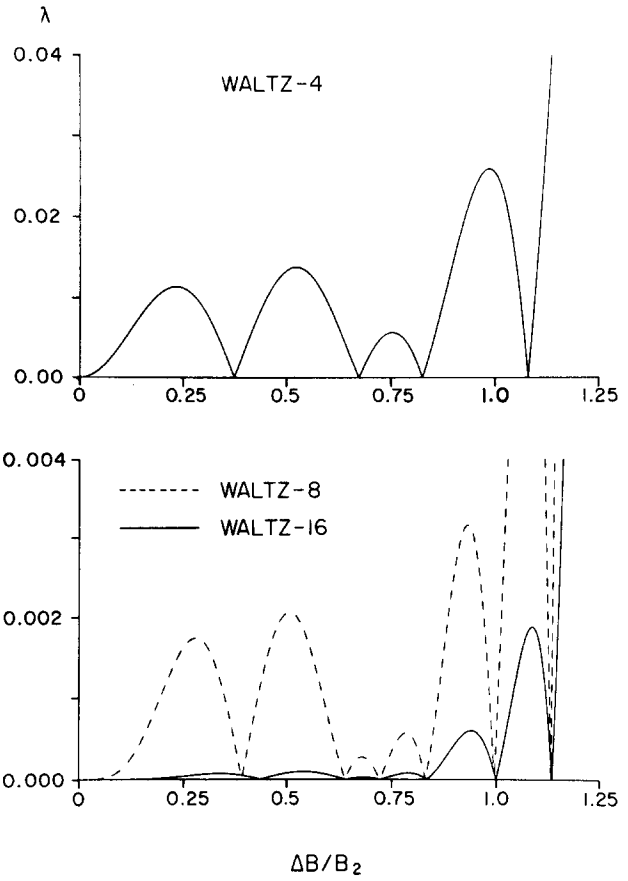

FIG. 7. Decoupling performance calculated for the WALTZ sequences in terms of the scaling parameter λ. Each stage of expansion gives an improvement of almost an order of magnitude. Note the tenfold expansion of the λ scale for the WALTZ-8 and WALTZ-16 sequences, where full scale represents only a 0.8 Hz residual splitting for J = 200 Hz.

the same phase, and which brings out the relationship with $R\bar{R}\bar{R}R$. Each unit K is a spin inversion sequence, having a better offset-dependence than the element R (Fig. 6). The decoupling performance of WALTZ-8 is illustrated in Fig. 7.

Once again the overall effect of the sequence is to induce a small rotation about an axis close to $+Z$. A similar procedure may be used for expansion to the next higher supercycle, by permuting a $90°(-X)$ pulse from the end to the beginning of the sequence, then appending a phase-inverted sequence, giving WALTZ-16

$$Q\bar{Q}\bar{Q}Q = \bar{3}4\bar{2}3\bar{1}2\bar{4}2\bar{3}\ 3\bar{4}2\bar{3}1\bar{2}4\bar{2}3\ 3\bar{4}2\bar{3}1\bar{2}4\bar{2}3\ \bar{3}4\bar{2}3\bar{1}2\bar{4}2\bar{3}. \quad [28]$$

Each unit Q is a good spin inversion sequence (Fig. 6) and the decoupling performance of the supercycle is further improved (Fig. 7). Note that Q may be derived directly from $RR\bar{R}\bar{R}$ simply by inverting the phase of the first 90° pulse

$$1\bar{2}3\ 1\bar{2}3\ \bar{1}2\bar{3}\ \bar{1}2\bar{3} \rightarrow \bar{3}42\bar{3}\bar{1}2\bar{4}2\bar{3} \quad [29]$$

in the same way that $1\bar{2}3$ was derived from $\bar{3}3$.

A disappointing aspect of the experimental tests was that the next stage of expansion WALTZ-32 did not show the expected improvement; further work on this aspect is in progress. It does, however, underline the danger of implicit reliance on computer simulations since there are many instrumental shortcomings which could degrade decoupling performance, particularly when the cycles become very long.

Spatial Inhomogeneity of the B_2 Field

The decoupling theory of Waugh (*11, 12*) can be used to provide insight into the effect of the spatial inhomogeneity of the B_2 field. This is actually in two parts: the direct influence of the B_2 distribution and the effect of motion of the sample through the inhomogeneous B_2 field, due to spinning. For simplicity only the first effect is considered here. Consider the simple sequence

$$R_X(\alpha_0)\bar{R}_X(\alpha_0) \quad [30]$$

where α_0 is the nominal flip angle on resonance ($\alpha = \alpha_0 \sec\theta$). The tilt angle of the effective field is given by $\tan\theta = \Delta B/B_2$. The effect of this pulse pair can be represented by the matrix $\mathbf{P}$

$$\mathbf{P} = \begin{bmatrix} A + iB & C \\ -C & A - iB \end{bmatrix} \quad [31]$$

where

$$A = 1 - 2\sin^2\theta\sin^2(\alpha/2)$$

$$B = 2\sin\theta\sin(\alpha/2)\cos(\alpha/2)$$

$$C = 2\sin\theta\cos\theta\sin^2(\alpha/2). \quad [32]$$

The overall effect of the pair of pulses is represented by a pure rotation of H_+ and H_- through the angles $\beta_\pm$ about the axes $\mathbf{n}_\pm$.

$$\cos 2\beta_\pm = \text{Trace}\{\mathbf{P}\}/2 = [1 - 2\sin^2\theta\sin^2(\alpha/2)] \quad [33]$$

If τ is the width of each pulse in seconds and $\omega = \gamma\Delta B$, then the scaling factor λ is given by (*11, 12*)

$$\lambda = (2\tau)^{-1}d\beta/d\omega = -(dA/d\omega)/[\tau(1 - A^2)^{1/2}]. \quad [34]$$

This is readily shown to give

$$\lambda = [\cos^3\theta\sin(\alpha/2)/(\alpha_0/2) + \sin^2\theta\cos(\alpha/2)][1 - \sin^2\theta\sin^2(\alpha/2)]^{-1/2}. \quad [35]$$

For the special case of irradiation at exact resonance ($\alpha = \alpha_0$), this simplifies to

$$\lambda = \sin(\alpha_0/2)/(\alpha_0/2). \quad [36]$$

Thus if $\alpha_0 = 180°$ then the scaling factor $\lambda = 2/\pi$, that is to say there is a large splitting $2J/\pi$ Hz. The sensitivity to B_2 inhomogeneity for the exact resonance case can be shown to be

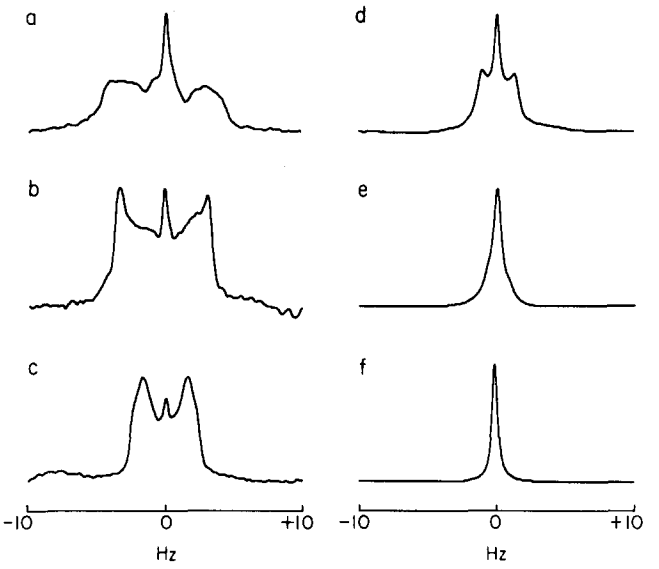

FIG. 8. Lineshapes distorted by B_2 inhomogeneity when the decoupling sequence $360n°(+X)\ 360n°(-X)$ is used. Intensities have been scaled to normalize the tallest peak. The number of revolutions per pulse is (a) 1 (b) 2 (c) 4 (d) 8 (e) 16, and (f) 32. Since the extent of the broadening depends on $\sin(\alpha_0/2)/(\alpha_0/2)$, the effect has just about disappeared in trace (f).

$$d\lambda/d\alpha_0 = [\alpha_0 \cos(\alpha_0/2) - 2\sin(\alpha_0/2)]/\alpha_0^2. \quad [37]$$

Thus the only conditions where the performance is insensitive to B_2 inhomogeneity are where α_0 is either very small or very large. Unfortunately in the limit of very small flip angle the sequence does not decouple ($\lambda \rightarrow 1$) so the only viable decoupling regime is where the flip angle is very large (several revolutions). This trend is apparent from the experimental results of Fig. 8, where the carbon-13 resonance of formic acid is studied for on-resonance decoupling with the square-wave modulation sequences

$$360n°(+X)\ 360n°(-X) \quad [38]$$

where n is 1, 2, 4, 8, 16, and 32 complete revolutions. The response consists of a narrow central line flanked by two much broader responses, the latter becoming less prominent as the flip angle is increased. When $n = 32$ revolutions the broad features have disappeared leaving a line less than 0.5 Hz wide. Related lineshape distortions with square-wave decoupling have been observed by Waugh (*14*). This gross effect of B_2 inhomogeneity explains why broadband decoupling by square wave modulation only works effectively at very low modulation frequencies where each "pulse" corresponds to many revolutions. In this limit, the term α_0^2 in the denominator ensures that the performance is quite insensitive to the exact setting of the flip angle.

The $180°(+X)\ 180°(-X)$ sequence can be put to good use in order to obtain a measure of the B_2 distribution in a practical case. Near the condition $\alpha_0 = \pi$ radians, not only is the observed splitting large, but it is also an almost linear function of flip

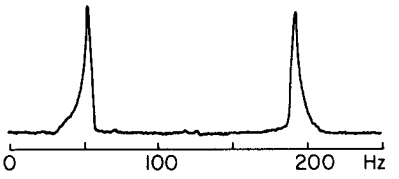

FIG. 9. Carbon-13 spectrum of formic acid "decoupled" by the sequence $180°(+X)\ 180°(-X)$ at exact resonance. The lineshape distortion is due to B_2 inhomogeneity and has been used to estimate the form of the B_2 distribution shown in Fig. 10. The instrument linewidth was only 0.2 Hz.

angle, which gives a virtually undistorted picture of the B_2 distribution curve. The protons of formic acid were irradiated at exact resonance and the carbon-13 spectrum examined. For a perfectly homogeneous B_2 field the observed splitting would be $2J_{CH}/\pi = 141$ Hz. The distorted lineshape can be seen in the spectrum of Fig. 9, and the B_2 distribution curve which can be extracted from the lineshape is illustrated in Fig. 10. Note that this distribution curve is automatically weighted according to the relative coupling of each volume element to the receiver coil. The effective homogeneity of B_2 for the Varian XL-200 broadband probe is in fact quite high, the points at which the signal strength falls to half maximum are separated by only 8.5% of the nominal B_2 intensity.

This information allows the decoupling behavior of WALTZ-16 to be recalculated to take B_2 inhomogeneity into account. The calculation is performed for a finite number of different volume elements, each with the appropriate values of α_0 and θ for a given resonance offset ΔB. The resulting carbon-13 spectrum is summed over all volume elements and convoluted with the usual Lorentzian lineshape function. The offset dependence is illustrated in Fig. 11a. Note that the main features of the experimental offset-dependence curve for formic acid (Fig. 11b) are clearly reproduced. There is a marked rounding of the shoulders of the curve and a perceptible

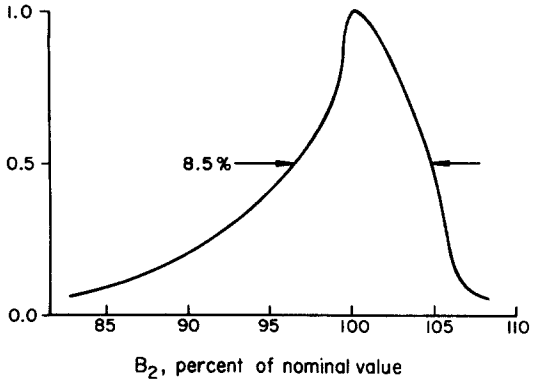

FIG. 10. The distribution of intensity of the B_2 field of a Varian XL-200 spectrometer measured from the double resonance experiment of Fig. 9. The ordinate represents the observed carbon-13 signal intensity (including a factor reflecting the coupling to the receiver coil).

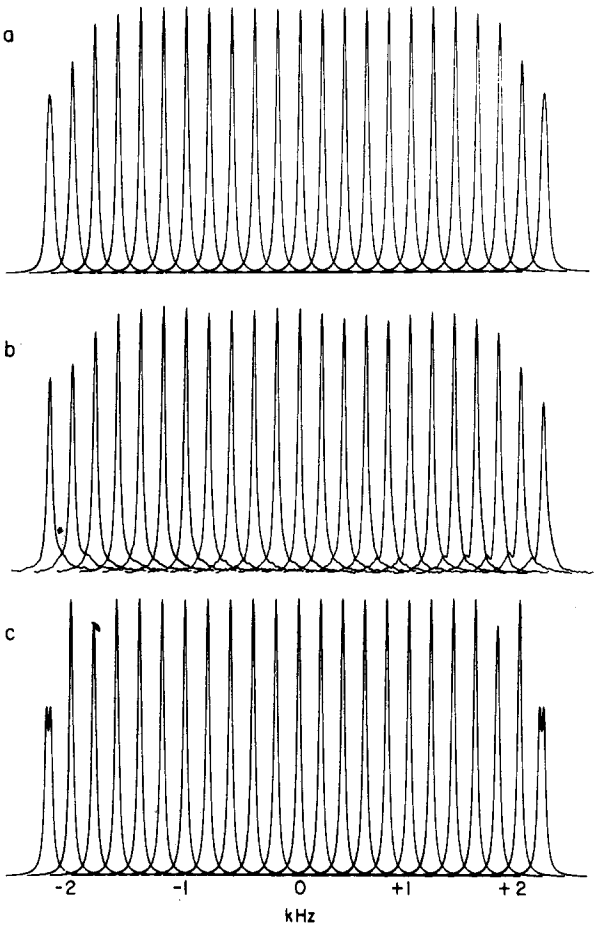

FIG. 11. WALTZ-16 decoupling of a carbon-13 resonance as a function of proton offset, in 200 Hz increments. (a) Computer simulation taking into account the measured B_2 inhomogeneity. (b) Experimental results for formic acid (J = 221 Hz). (c) Computer simulation assuming a perfectly uniform B_2 field. In all these spectra, $\gamma B_2/2\pi$ = 2kHz and the line broadening is 0.25 Hz.

broadening of the resonances at the extremes of the offset range. Simulations which do not take B_2 inhomogeneity into account are shown for comparison (Fig. 11c); the behavior at the edges of the effective bandwidth is quite different, even to the extent that a well-resolved residual splitting is predicted at the largest offset.

This method of mapping the B_2 distribution appears to be much simpler to put into practice than earlier methods based on exploration with a small probe sample using spin tickling (*22, 23*). Clearly B_2 inhomogeneity is one of the principal instrumental factors which intervenes to make experimental decoupling performance less uniform than the idealized calculations predict. Hence the danger of using the idealized simulations alone for predicting decoupling performance.

Motion of the sample through the inhomogeneous B_2 field is more difficult to treat. It is clear that sample spinning is a slow process on the time scale of the proton

decoupler cycling. Since the actual B_2 distribution measured above is relatively narrow, it is tempting to assume that such spinning effects will not be too serious.

Pulse Length Adjustment

Tolerance of small errors in the nominal flip angles is important for practical applications of decoupling. In the first place an accurate calibration of the B_2 intensity is difficult, partly because of B_2 inhomogeneity which broadens and distorts the lines. In the second place the nature of the sample itself influences the actual B_2 intensity particularly if ionic solutions are used, as in many biochemical investigations.

Once the decoupling sequence has been programmed (or hardwired), the flip angle adjustment is the only calibration required. It is usually carried out by first calibrating $\gamma B_2/2\pi$ in hertz by measuring the residual splittings in a series of coherent off-resonance decoupling experiments with a sample of known J_{CH}. Measurements are made on both sides of resonance so that the exact resonance condition can be pinpointed and ΔB values determined. The observed residual splitting S is given by the formula (*1, 17*)

$$S \cong J_{CH}\Delta B/(B_2^2 + \Delta B^2)^{1/2}. \qquad [39]$$

For situations where the offsets are not too large ($B_2 \gg \Delta B$), the approximate formula can be used (*1*)

$$S \cong J_{CH}\Delta B/B_2. \qquad [40]$$

If the splitting is measured by taking the peaks of the two resonance lines to be their centers, then this method measures B_2 at the peak of the B_2 distribution curve, the most probable value. Once B_2 has been calibrated it is usually necessary to reset it to a suitable level for decoupling without overheating the sample. (In the present experiments the chosen condition was $\gamma B_2/2\pi = 2$ kHz). A new calibration is then performed and then the pulse widths set to the required conditions

$$\gamma B_2 t_1 = \pi/2$$

$$\gamma B_2 t_2 = \pi$$

$$\gamma B_2 t_3 = 3\pi/2. \qquad [41]$$

In practice the WALTZ-16 sequence possesses a built-in compensation for small errors in these flip angles. This is most easily shown by computer simulation of the decoupling performance for sequences where all three flip angles have been decreased or increased in the same proportion. For this purpose the offset dependence of the residual carbon-13 splittings provides a suitable test, bearing in mind that any splittings that are less than 0.1 Hz will not significantly affect the peak height of the carbon-13 resonance. Figures 12 and 13 compare the curves for correctly set pulse lengths with those calculated for a 5% decrease and increase in the nominal flip angles. Note that the sequence is somewhat more tolerant of increases in the flip angles in the range $-B_2 < \Delta B < +B_2$. For this reason, and because of the skewed B_2 distribution, it is a good practice to set the nominal flip angles a few percent high.

The two radiofrequency channels must of course be properly balanced in ampli-

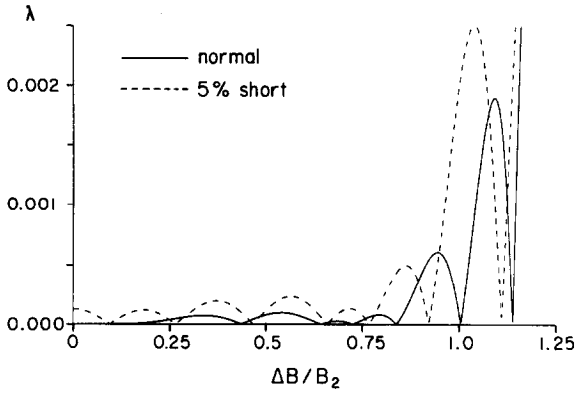

FIG. 12. Effect of short radiofrequency pulses in the WALTZ-16 decoupling sequence. Calculated scaling factor λ versus offset parameter for correctly calibrated pulse lengths, and for the case that all pulses are 5% short. Full scale on the λ axis corresponds to a residual splitting of 0.5 Hz for J = 200 Hz.

tude. Computer simulations suggest that an imbalance of the order 0.5% would just produce a perceptible degradation of decoupling performance near the shoulders of the offset-dependence curve. Fortunately in most spectrometers the 0 and 180° signals are generated at an early stage of the radiofrequency circuit and the final amplifiers operate in Class C. Consequently the two channels are likely to be closely balanced.

Radiofrequency Phase

The strong point of the sequences proposed by Waugh (*11, 13*) and the WALTZ sequences described here is that they require only two radiofrequency phases (0 and 180°) and that they are insensitive to errors in this phase shift, in contrast to the MLEV sequences. It can be shown analytically that any sequence $A\bar{B}$ is quite tolerant of errors in the 180° phase shift.

Suppose that A and B are rotation operators describing rotations about the usual tilted effective fields in the proton rotating frame, and having the same phase and arbitrary nominal flip angles at exact resonance. If a sequence $A\bar{B}$ is constructed, the overall rotation β depends only on

$$\text{Trace}\{A\bar{B}\} \qquad [42]$$

If the radiofrequency phase is incorrectly adjusted by a small angle δ then this becomes

$$\text{Trace}\{A\,R_Z(\delta)\,\bar{B}\,R_Z(-\delta)\} \qquad [43]$$

where $R_Z(\delta) = \exp(i\delta I_Z)$ is a rotation through an angle δ about the Z axis. For spin-½ nuclei this may be expanded to first order

$$R_Z(\delta) \cong \mathbb{1} + i\delta I_Z = \mathbb{1} + (\delta/2)\exp(i\pi I_Z) = \mathbb{1} + (\delta/2)R_Z(\pi). \qquad [44]$$

This permits the approximation

$$\text{Trace}\{A\,R_Z(\delta)\,\bar{B}\,R_Z(-\delta)\}$$

$$\cong \text{Trace}\{A\bar{B}\} + \text{Trace}\{(1/2)\delta[A\,R_Z(\pi)\,\bar{B} - A\,\bar{B}\,R_Z(\pi)]\} \qquad [45]$$

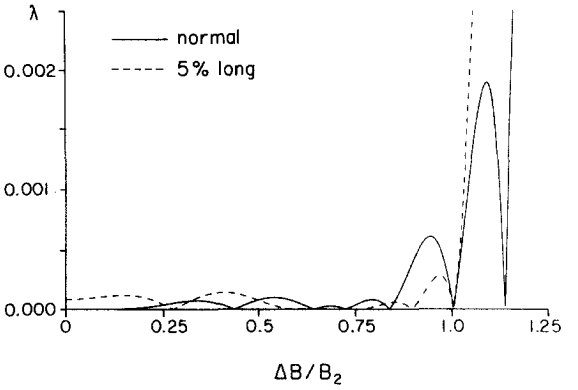

FIG. 13. Effect of long radiofrequency pulses. Calculated scaling factor λ versus offset parameter for correctly calibrated pulse lengths, and for the case that all pulses are 5% long. Note that for offsets up to $\Delta B = B_2$, the WALTZ-16 sequence is more tolerant of increases than decreases in pulse lengths.

neglecting higher-order terms in δ. The sequence is thus insensitive to small phase errors if the second term vanishes. Now,

$$\begin{aligned}\text{Trace}\{A\,\bar{B}\,R_Z(\pi)\} &= \text{Trace}\{A\,R_Z(\pi)\,B\,R_Z(-\pi)R_Z(\pi)\}\\ &= \text{Trace}\{A\,R_Z(\pi)\,B\}.\end{aligned} \quad [46]$$

Since the trace is invariant under cyclic permutation, this equals

$$\begin{aligned}\text{Trace}\{(A+B)R_Z(\pi)\} &= \text{Trace}\{A\,R_Z(\pi)\,R_Z(-\pi)\,B\,R_Z(\pi)\}\\ &= \text{Trace}\{A\,R_Z(\pi)\,\bar{B}\}.\end{aligned} \quad [47]$$

Consequently

$$\text{Trace}\{A\,R_Z(\delta)\,\bar{B}\,R_Z(-\delta)\} \cong \text{Trace}\{A\bar{B}\} \quad [48]$$

so the decoupling behavior is insensitive to phase errors δ to first order in δ.

Confirmation for more complicated sequences is obtained by recalculating the decoupling performance for a deliberately misadjusted radiofrequency phase shift (Fig. 14) showing that errors of 10° have little effect on the offset-dependence curve.

Phase Transients

Radiofrequency pulses require a perceptible time for the current to rise or fall in the NMR coil, which is usually part of a tuned resonant circuit. It has been shown (*24, 25*) that this introduces an effect equivalent to a momentary shift of the radiofrequency phase, the so-called "phase glitch." Even where the edges of the "pulse" are defined by the inversion of the radiofrequency phase (as in the present experiments), in practice this usually means that one radiofrequency channel is switched off a short time before the other channel is switched on, so similar phase transients may be anticipated. This phase glitch effect is particularly serious in solid state NMR experiments where the pulses are very short (of the order of a microsecond or less). The present decoupling experiments employ much longer pulses (of the order of 100 μsec) so the problem should be correspondingly less severe.

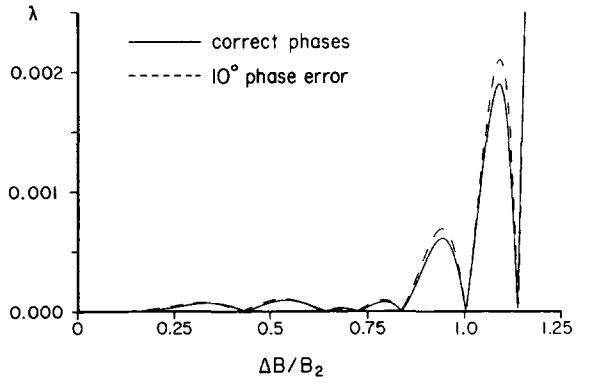

FIG. 14. Tolerance of radiofrequency phase error in the WALTZ-16 sequence. Calculated scaling factors λ for exact 180° phase shift between channels, and a 170° phase shift. The decoupling performance is not affected significantly.

Computer simulations were nevertheless carried out to explore the expected magnitude of the phase transient effect with the WALTZ-16 broadband decoupling sequence. The perturbation of the motion of the proton spins is taken to be equivalent to the effect of introducing two fictitious short pulses, one just before and one just after the main pulse, and both in quadrature with respect to the main pulse. Both the symmetric combination (both fictitious pulses in phase) and the corresponding antisymmetric combination were considered. Experimental observations on the Varian XL-200 spectrometer indicated that the equivalent fictitious pulses were of the order of 0.3 μsec. Since they were reproducible and unaffected by probe tuning or radiofrequency level, they probably originated in the earlier radiofrequency circuitry rather than in the tuned decoupler coil. The scaling factors λ computed for WALTZ-16, including 1 μsec fictitious pulses representing the effect of phase transients, were not significantly worse than those calculated for perfectly rectangular pulses, and it was therefore concluded that these effects can most likely be neglected in practical decoupling situations.

Cycling Sidebands

One inevitable shortcoming of cyclically modulated decoupling sequences is the appearance of weak sidebands in the decoupled spectrum at the cycling rate and its harmonics. If it is possible to introduce a random timing into the experiment then these sidebands can be spread out into a very broad weak feature that would be lost in the baseline noise, which is what happens in the case of conventional noise decoupling. A partial cancellation of cycling sidebands can be achieved with composite pulse decoupling by desynchronizing the proton pulse timing and the carbon-13 data acquisition rate. If this is followed by a time-averaging process many of the cycling sidebands have random phases and tend to cancel out. Others persist but with reduced intensity.

To facilitate this cancellation process, a hardwired WALTZ-16 decoupler was con-

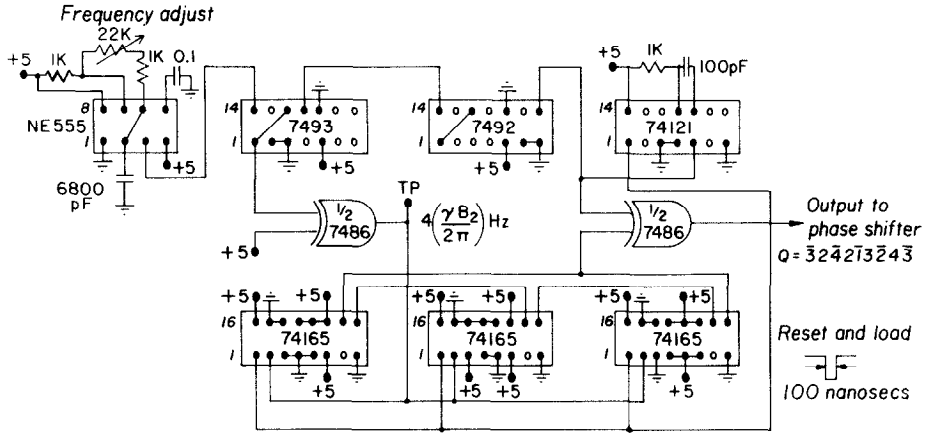

FIG. 15. Schematic circuit diagram of the hardwired version of the WALTZ-16 decoupler. For description see Appendix.

structed which ran from an internal clock that was out of synchronism with the computer-controlled carbon-13 acquisition rate. The circuit is set out in Fig. 15, and a brief description appears in the Appendix. The clock rate is the parameter which determines the pulse widths t_1, t_2, and t_3, and it is set up to generate the frequency $4(\gamma B_2/2\pi)$ Hz once B_2 has been calibrated as described above.

With this asynchronous decoupling mode the level of cycling sidebands was tested experimentally with the WALTZ-16 sequence. The number and intensity of cycling sidebands depend on the proton resonance offset. Measurements were made on a Varian XL-200 spectrometer (with $\gamma B_2/2\pi$ = 2 kHz) at exact proton resonance and offsets of 500, 1000, 1500, and 2000 Hz (Fig. 16). Only at the 2000 Hz offset, which is just outside the usable bandwidth, were the sidebands intense enough to cause any practical concern. For the other offsets the sidebands were always less than 0.3% of the central decoupled resonance. Rather surprisingly, there are more cycling sidebands observed for decoupling at exact resonance than at some other offsets.

Cycling sidebands could prove a particularly critical problem in experiments designed to observe carbon–carbon coupling in natural abundance samples. However, it has been demonstrated experimentally that with the systematic procedures for phase cycling used in the "INADEQUATE" experiment (*26*) the intensity of the cycling sidebands is essentially negligible in comparison with that of the carbon-13 satellites. This is because the cycling sidebands with random phase are averaged out after many transients, while those with coherent phase are removed by the phase-cycling procedure which cancels the strong "parent" carbon-13 resonance. Thus both spinning sidebands and cycling sidebands disappear. A spectrum from *N*-acetyl-3,4-dimethylaniline is shown in Fig. 17. The cycling sidebands have been reduced to a very low intensity indeed. This is a good example of a situation where high resolution is required even though broadband proton decoupling is being used. When conventional square-wave decoupling (*2*) was employed for this experiment only poor resolution was achieved. The investigation of coupling between carbon-13 and deuterium (or some other heteronuclear species) would similarly require high resolution conditions.

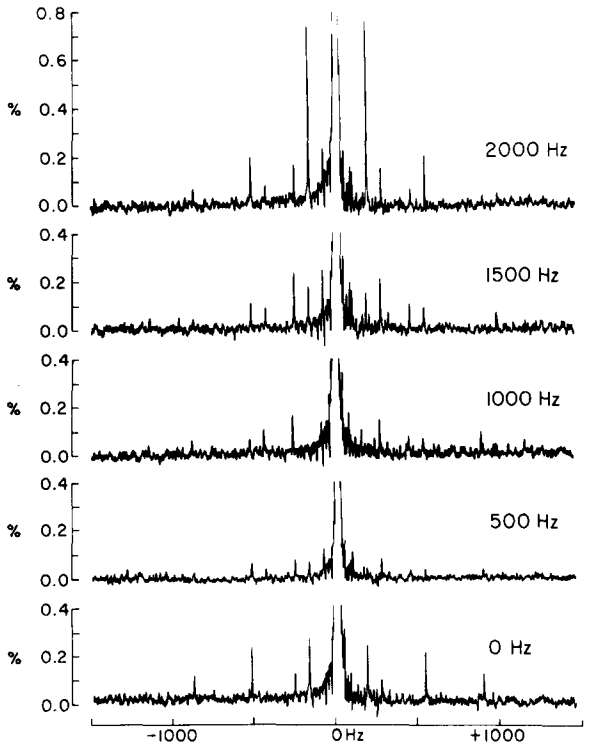

FIG. 16. Cycling sidebands observed with the WALTZ-16 decoupling sequence at various offsets from exact proton resonance ($\gamma B_2/2\pi$ = 2 kHz). A hardwired (asynchronous) decoupler was used; 512 transients were accumulated. The intensity scales are calibrated as a percentage of the peak height of a coherently decoupled carbon-13 resonance. Note that the offset 2000 Hz is just outside the normal operating bandwidth of the decoupler.

Scope for Improvement

Much has been made of the self-compensating properties of a 90° pulse, on the one hand for constructing a new spin-inversion element, and on the other hand for ensuring that the pulse which is cyclically permuted is reasonably close to ideality. One direction for improvement is to design a composite 90° pulse, a concept that has been explored earlier (*20*). This is achieved very simply with the sequence

$$a°(-X)\,(90 + a)°(+X) \qquad [49]$$

where a is a relatively small angle compared with 90°. In practice the condition a = 22.5° was adopted to simplify the generation of sequences by digital methods. The improvement over a simple 90° pulse may be appreciated from Fig. 18, where the residual Z components are plotted against resonance offset; the composite pulse leaves a Z component which is always appreciably smaller.

In this way it is possible to convert the element $R = 1\bar{2}3$ into a new element S by modifying the initial and final 90° pulses

$$S = 22.5°(-X)\ 112.5°(+X)\ 180°(-X)\ 292.5°(+X)\ 22.5°(-X). \qquad [50]$$

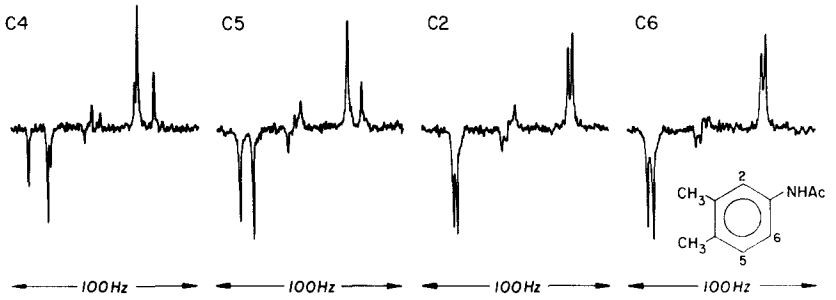

FIG. 17. Natural-abundance carbon-13 spectrum of *N*-acetyl-3,4-dimethylaniline showing the C4, C5, C2, and C6 regions on an expanded frequency scale. The "INADEQUATE" technique has been used to suppress the strong resonances from isolated carbon-13 spins, leaving the pattern of carbon-carbon splittings (relative intensity 0.5%). This is used as an illustration of the fact that WALTZ-16 broadband decoupling ($\gamma B_2/2\pi$ = 2 kHz) does not introduce cycling sidebands of appreciable intensity on this scale. Proton decoupling and carbon-13 sampling were asynchronous.

Introducing a shorthand notation where italic numerals represent rotations *in units of 22.5 degrees* this may be written

$$S = \bar{1}\,5\,\bar{8}\,13\,\bar{1}. \qquad [51]$$

An important attribute of this sequence is an additional maximum in the curve of inversion efficiency against offset, at offsets beyond $\Delta B = +B_2$ where the simple element $R = 1\bar{2}3$ begins to roll off. Hence the effective bandwidth can be improved.

Extended supercycles are constructed in exactly the same fashion as the WALTZ sequences, except that it is the composite element $1\bar{5}$ which is cyclically permuted instead of a simple 90° pulse. Thus the first stage of expansion gives

$$SS\bar{S}\bar{S} = \bar{1}\,5\,\bar{8}\,13\,\bar{1}\;\;\bar{1}\,5\,\bar{8}\,13\,\bar{1}\;\;1\,\bar{5}\,8\,\bar{13}\,1\;\;1\,\bar{5}\,8\,\bar{13}\,1. \qquad [52]$$

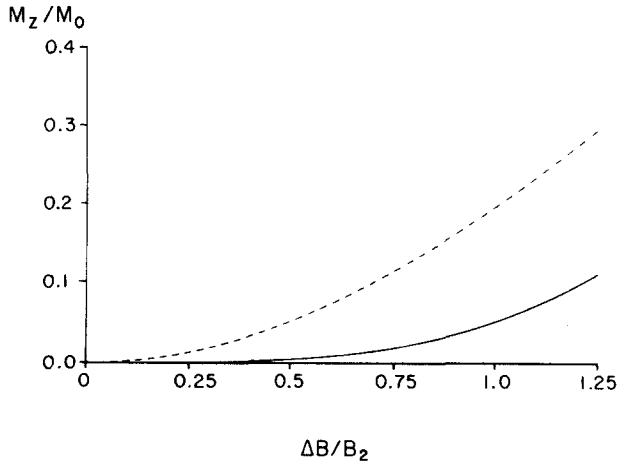

FIG. 18. The residual Z component of magnetization as a function of offset for a simple 90° pulse (dashed line) and the composite sequence 22.5°($-X$) 112.5°($+X$) (solid line).

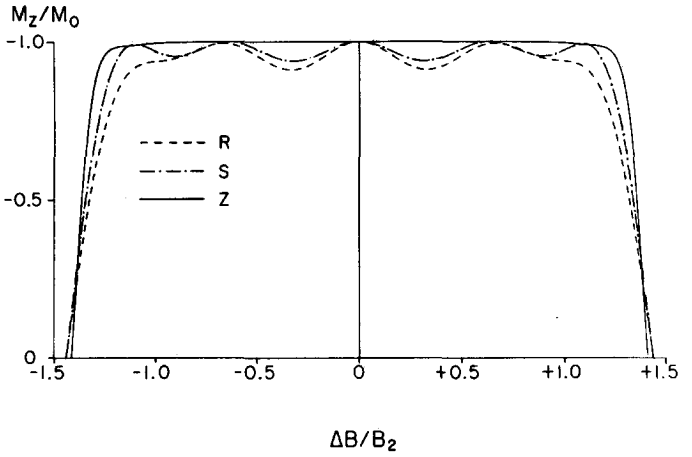

FIG. 19. Efficiency of composite pulse sequences for inversion of Z magnetization. The sequence $R = 1\bar{2}3$ is the least effective, while $S = \bar{1}5\bar{8}13\bar{1}$ exhibits new maxima near $\Delta B = \pm 1.1\ B_2$ at the edges of the effective bandwidth. Expansion to the sequence $Z = 1\,\overline{13}\,13\bar{2}5\bar{8}13\bar{1}\,1\bar{5}8\,\overline{13}\,2\bar{5}8\,\overline{13}\,1$ gives the very flat response traced out by the full curve.

Cyclic permutation of $\bar{1}5$ from left to the right gives

$$L\bar{L}\bar{L}L \text{ where } L = \bar{8}\,13\bar{2}5\bar{8}13\bar{1}\,1\bar{5} \qquad [53]$$

and further expansion by cyclic permutation of $1\bar{5}$ from right to left gives

$$Z\bar{Z}\bar{Z}Z \text{ where } Z = 1\,\overline{13}\,13\bar{2}5\bar{8}13\bar{1}\,1\bar{5}8\,\overline{13}\,2\bar{5}8\,\overline{13}\,1. \qquad [54]$$

The element Z should be an exceedingly effective spin inversion sequence over an offset range $-1.4B_2 < \Delta B < +1.4B_2$ (see Fig. 19). The supercycle $Z\bar{Z}\bar{Z}Z$ is only 17% longer than WALTZ-16, but its performance is predicted to be superior, the computed scaling factors and residual splittings being quite negligible over the range $-1.25\ B_2 < \Delta B < +1.25\ B_2$ (Fig. 20). This does not of course guarantee a correspondingly high performance in practice; the sequence might be more sensitive to the effects of phase transients ("phase glitch") since it incorporates many more inversions of the radiofrequency phase, and pulses of small flip angle. Some early exploratory experiments have so far proved disappointing.

CONCLUSIONS

Not all decoupling applications call for the high resolution conditions described in this paper; often linewidths of the order of 1 Hz would be acceptable for routine carbon-13 spectroscopy. However, when there is fine structure on the carbon-13 lines due to coupling to nuclei other than protons, access to higher resolving power may be very important, and then the WALTZ-16 sequence is expected to be preferable to earlier low-power decoupling sequences. The new scheme has the advantage of an effective bandwidth very similar to that of MLEV-64 for the same B_2 level, but it is far less sensitive to the setting of the radiofrequency phase, indeed it needs only two radiofrequency channels (0 and 180°) and it is consequently simpler to implement. None of the other decoupling features are in any way inferior to those of the MLEV-sequences, and it may be concluded that the WALTZ-16 scheme is to be preferred.

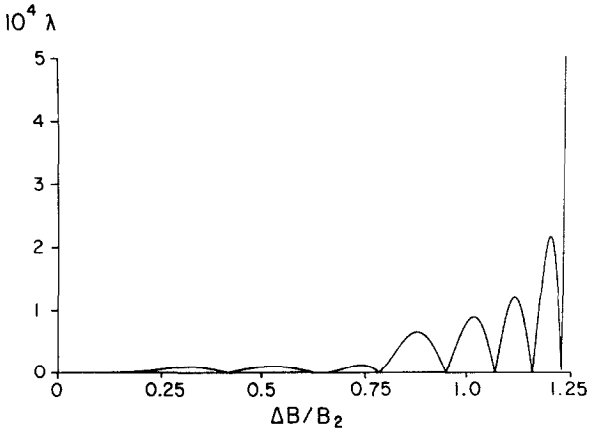

FIG. 20. Simulated decoupling performance for the sequence $Z\bar{Z}\bar{Z}Z$ as a function of proton resonance offset. Note particularly the very small scaling factors λ, full scale representing only a 0.1 Hz residual splitting for J = 200 Hz.

APPENDIX

A "Blackbox" Decoupler

The hardwired decoupler circuit is shown in Fig. 15. The heart of the design is a 24-bit shift register made up from three 8-bit registers connected in a loop. If the WALTZ-16 sequence is written $QQ\bar{Q}\bar{Q}$ then each section Q consists of twenty-four 90° pulses; the shift register is thus wired up with the sequence Q (a 0 representing a pulse along the $+X$ axis, a 1 representing a pulse along $-X$), and is advanced at a rate $4(\gamma B_2/2\pi)$ Hz. In the circuit shown in Fig. 15, the sequence Q is in fact generated in a time-reversed order. This has no influence on the operation of the decoupler. It is a general property of sequences which use only 0° and 180° phases that decoupling is unaffected by reversing the order of the pulses. Combination of the output of the shift register with a logic signal from the clock at $(\gamma B_2/2\pi)/24$ Hz in an exclusive OR gate generates the sequence $QQ\bar{Q}\bar{Q}$.

The NE555 clock is free running at $8(\gamma B_2/2\pi)$ Hz and is followed by a divide-by-two circuit and an inverter (since the shift register advances on a *rising* edge). The clock frequency is adjusted by means of the multiturn 22K potentiometer while observing the test point (TP) waveform on an oscilloscope. This adjustment requires a prior calibration of the B_2 intensity as described in the text. The remainder of the 7493 device and the 7492 device provide the required division by 8 and by 12.

It is essential to synchronize the start of the sequence Q with the edges of the clock pulses at $(\gamma B_2/2\pi)/24$. This is achieved by converting the rising edges of the slow clock pulses into 100 nsec "load and reset" pulses (in the 74121 monostable) which causes the Q sequence to be reloaded into the shift register. This operation is very much faster than the elements of the sequence Q and therefore does not influence its timing.

The construction uses a double-sided circuit board, one side being a continuous ground plane. Each chip is decoupled with a 0.01 μF ceramic disc capacitor close to its +5 V supply pin. The output is fed directly to the existing Varian XL-200 phase shifter. Alternatively, with the aid of a suitable "totem pole" driver, it could generate the phase shifts via a double-balanced mixer.

ACKNOWLEDGMENTS

This investigation was made possible by an equipment grant from the Science and Engineering Research Council and was supported by a Rhodes Scholarship and NCAA Postgraduate Fellowship (A.J.S.), and a Domus Senior Scholarship from Merton College (J.K.). The rationale for describing the sequence $R = \bar{1}23$ in terms of $90°(+X)\ [90°(-X)]^{-1}$ was suggested by M. H. Levitt during a visit to this laboratory. These experiments owe a considerable debt to earlier careful practical work on cyclic decoupling sequences by T. Frenkiel. A preliminary description of the WALTZ-16 sequence has been submitted to this *Journal* (*18*).

Note added in proof. Subsequent experimental and theoretical work has shown that amplitude imbalance between the 0 and 180° channels is one of the principal reasons why the expansion from WALTZ-16 to WALTZ-32 did not exhibit the expected improvement in decoupling performance. (This is a general property of all such sequences.) Although WALTZ-16 tolerates a channel imbalance of up to 0.5% without a serious degradation in performance, WALTZ-32 is much more sensitive to this kind of imperfection. At this stage in the expansion, amplitude imbalance has a relatively large influence on the direction of the overall rotation axis of the sequence, turning it away from the Z axis; this type of error is not compensated. With careful adjustment of the amplitude balance, the performance of WALTZ-32 becomes comparable with that of WALTZ-16 but it does not reach the theoretically predicted performance.

These results have important implications if double-balanced mixers are used to generate the 180° decoupler phase shifts, since the amplitude balance may then be inadequate unless it is adjusted experimentally using the linewidth of a decoupled carbon-13 line as the criterion.

REFERENCES

1. R. R. ERNST, *J. Chem. Phys.* **45,** 3845 (1966).
2. J. B. GRUTZNER AND R. E. SANTINI, *J. Magn. Reson.* **19,** 173 (1975).
3. V. J. BASUS, P. D. ELLIS, H. D. W. HILL, AND J. S. WAUGH, *J. Magn. Reson.* **35,** 19 (1979).
4. R. W. DYKSTRA, *J. Magn. Reson.* **46,** 503 (1982).
5. U. HAEBERLEN AND J. S. WAUGH, *Phys. Rev.* **175,** 453 (1968).
6. M. H. LEVITT AND R. FREEMAN, *J. Magn. Reson.* **43,** 502 (1981).
7. M. H. LEVITT, R. FREEMAN, AND T. FRENKIEL, *J. Magn. Reson.* **47,** 328 (1982).
8. M. H. LEVITT, R. FREEMAN, AND T. FRENKIEL, *J. Magn. Reson.* **50,** 157 (1982).
9. M. H. LEVITT, R. FREEMAN, AND T. FRENKIEL, "Advances in Magnetic Resonance" (J. S. Waugh, Ed.) Academic Press, New York, in press.
10. M. H. LEVITT, R. FREEMAN, AND T. FRENKIEL, 23rd Experimental NMR Conference, Madison, Wisconsin, 1982.
11. J. S. WAUGH, *J. Magn. Reson.* **49,** 517 (1982).
12. J. S. WAUGH, *J. Magn. Reson.* **50,** 30 (1982).
13. F. S. DEBOUREGAS, 23rd Experimental NMR Conference, Madison, Wisconsin, 1982.
14. J. S. WAUGH, private communication.
15. R. FREEMAN, T. FRENKIEL, AND M. H. LEVITT, *J. Magn. Reson.* **50,** 345 (1982).
16. A. L. BLOOM AND J. N. SHOOLERY, *Phys. Rev.* **97,** 1261 (1955).
17. W. A. ANDERSON AND R. FREEMAN, *J. Chem. Phys.* **37,** 85 (1962).
18. A. J. SHAKA, J. KEELER, T. FRENKIEL, AND R. FREEMAN, *J. Magn. Reson.* **52,** 335 (1983).
19. R. FREEMAN AND H. D. W. HILL, *J. Chem. Phys.* **54,** 3367 (1971).
20. R. FREEMAN, S. P. KEMPSELL, AND M. H. LEVITT, *J. Magn. Reson.* **38,** 453 (1980).
21. M. H. LEVITT, *J. Magn. Reson.* **50,** 95 (1982).
22. R. FREEMAN AND W. A. ANDERSON, *J. Chem. Phys.* **37,** 2059 (1962).
23. R. FREEMAN, J. B. GRUTZNER, G. A. MORRIS, AND D. L. TURNER, *J. Am. Chem. Soc.* **100,** 5637 (1978).
24. J. D. ELLETT, M. G. GIBBY, U. HAEBERLEN, A. PINES, AND J. S. WAUGH, "Advances in Magnetic Resonance" (J. S. Waugh, Ed.), Vol. 5, p. 117, Academic Press, New York, 1971.
25. M. MEHRING AND J. S. WAUGH, *Rev. Sci. Instrum.* **43,** 649 (1972).
26. A. BAX, R. FREEMAN, AND S. P. KEMPSELL, *J. Am. Chem. Soc.* **102,** 4849 (1980).